Supplement of Atmos. Chem. Phys., 25, 7647–7667, 2025
https://doi.org/10.5194/acp-25-7647-2025-supplement
© Author(s) 2025. CC BY 4.0 License.

Supplement of

Physical processes influencing the Asian climate due to black carbon emission over East Asia and South Asia

Feifei Luo et al.

Correspondence to: Feifei Luo (lff@cuit.edu.cn)

The copyright of individual parts of the supplement might differ from the article licence.

Table S1. Details of the five models in the PDRMIP project

Model	Resolution (lonxlat)	Aerosol setup	Indirect effects included
CESM1-CAM5	2.5°x1.9° 30 levels	CMIP5 Emissions (year 2005)	All indirect effects
GISS-E2-R	2.5°x2° 40 levels	AeroCom Phase II concentrations	no indirect effects
HadGEM3	1.875°x1.25° 85 levels	AeroCom Phase II concentrations	no indirect effects
MIROC-SPRINTARS	1.4°x1.4° 40 levels	HTAP2 emissions (year 2010)	All indirect effects
NorESM1	2.5°x1.9° 26 levels	AeroCom Phase II concentrations	All indirect effects

Table S2. Area-averaged responses for net TOA and surface energy over East China in BC_CHI and BC_CHI+IND, and over India in BC_IND and BC_CHI+IND. Positive values mean downward for radiation and flux changes. Responses significant above the 95% level are shown in bold. Unit: W/m^2

	BC_CHI (20°N-53°N,95°E-133°E)			**BC_IND** (5°N-35°N,65°E-95°E)			**BC_CHI+IND** (20°N-53°N,95°E-133°E)/ (5°N-35°N,65°E-95°E)		
	DJF	MAM	SON	DJF	MAM	SON	DJF	MAM	SON
TOA SW	**4.21**	**8.91**	**4.52**	**4.08**	**6.96**	4.39	**4.59/4.57**	**8.75/7.51**	4.24/**5.63**
SW	**-16.2**	**-30.03**	**-17.49**	**-23.57**	**-27.80**	**-23.35**	**-15.80/-23.26**	**-31.0/-28.13**	**-17.98/-23.26**
LW	-4.16	**-6.87**	**-4.76**	-1.21	-0.98	-3.26	-4.18/-1.11	-5.6/0.19	**-5.0**/-2.55
SH	**6.14**	**9.26**	**5.36**	**6.55**	**10.86**	**6.78**	**6.73/6.66**	**9.48/10.37**	**6.09/7.16**
LH	**8.29**	13.45	11.75	12.42	5.62	**11.12**	**9.36/12.94**	**14.02**/4.88	11.35/9.89

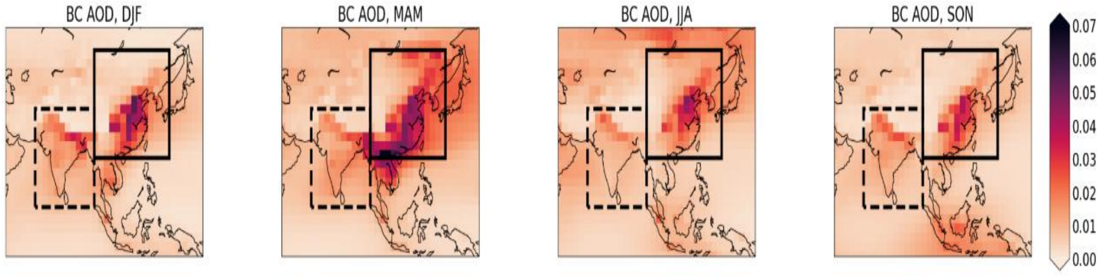

Figure S1. Spatial patterns of seasonal AOD of BC within China (CHI, solid) and India (IND, dashed).

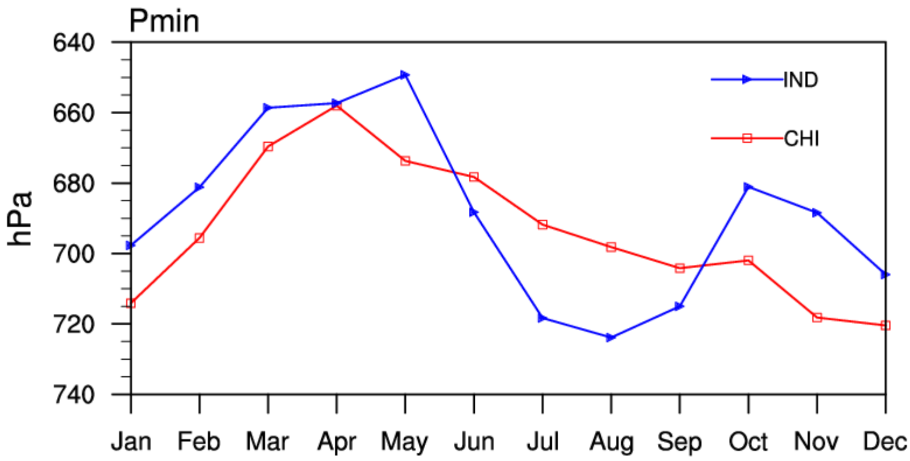

Figure S2. Seasonal evolutions of the regional mean p_{min} for China (red line, CHI, the solid box in Fig. S1), and India (blue line, IND, the dashed box Fig. S1).

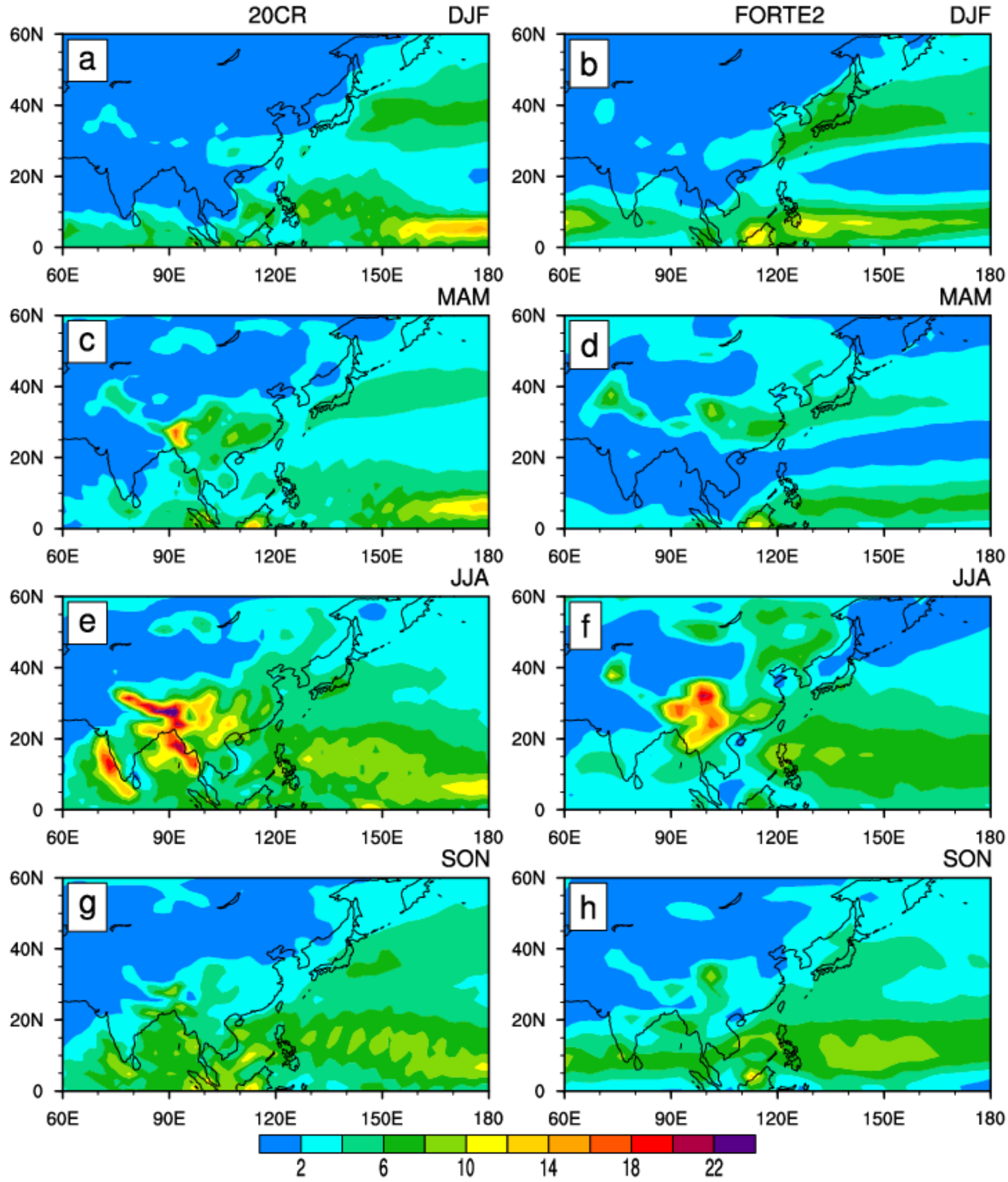

Figure S3. Climate state of precipitation in (left) 20CR and (right) the baseline simulation of FORTE2 in (a-b) DJF, (c-d) MAM, (e-f) JJA and (g-h) SON. Unit: mm/day

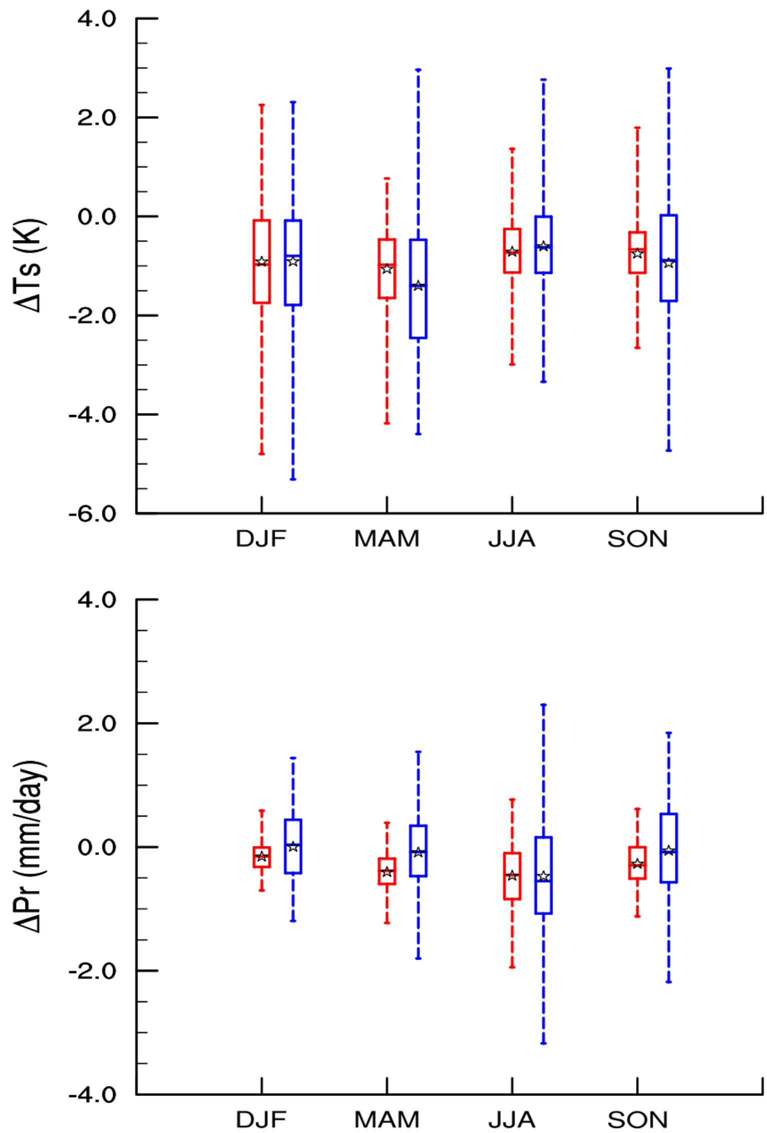

Figure S4. Box and Whisker plots showing the distributions of (upper) Ts and (lower) Pr differences between the perturbation simulations and baseline simulation. Boxes mean the interquartile range of differences; lines within the boxes mean the median; whiskers mean the minimum and maximum values, respectively; Stars show the average value. Red box and whisker plots represent area-averaged differences between BC_CHI and piC over East China. Blue box and whisker plots represent area-averaged differences between BC_IND and piC over India.

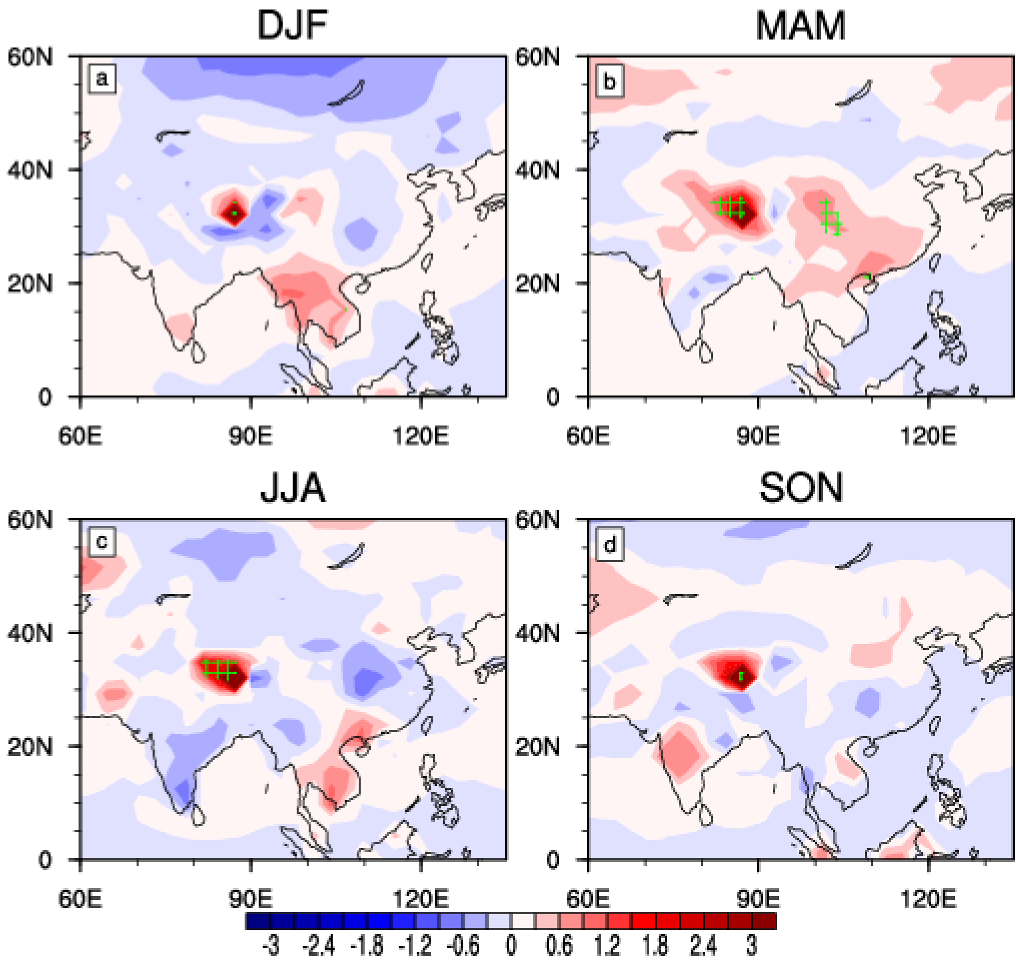

Figure S5. The linearity of Ts responses to Asian BC aerosol in four seasons [BC_CHI+IND-(BC_CHI+BC_IND)]. The green gridlines indicate the regions where the responses are statistically significant above 95% level based on a two-tailed Student's t-test. Unit: K

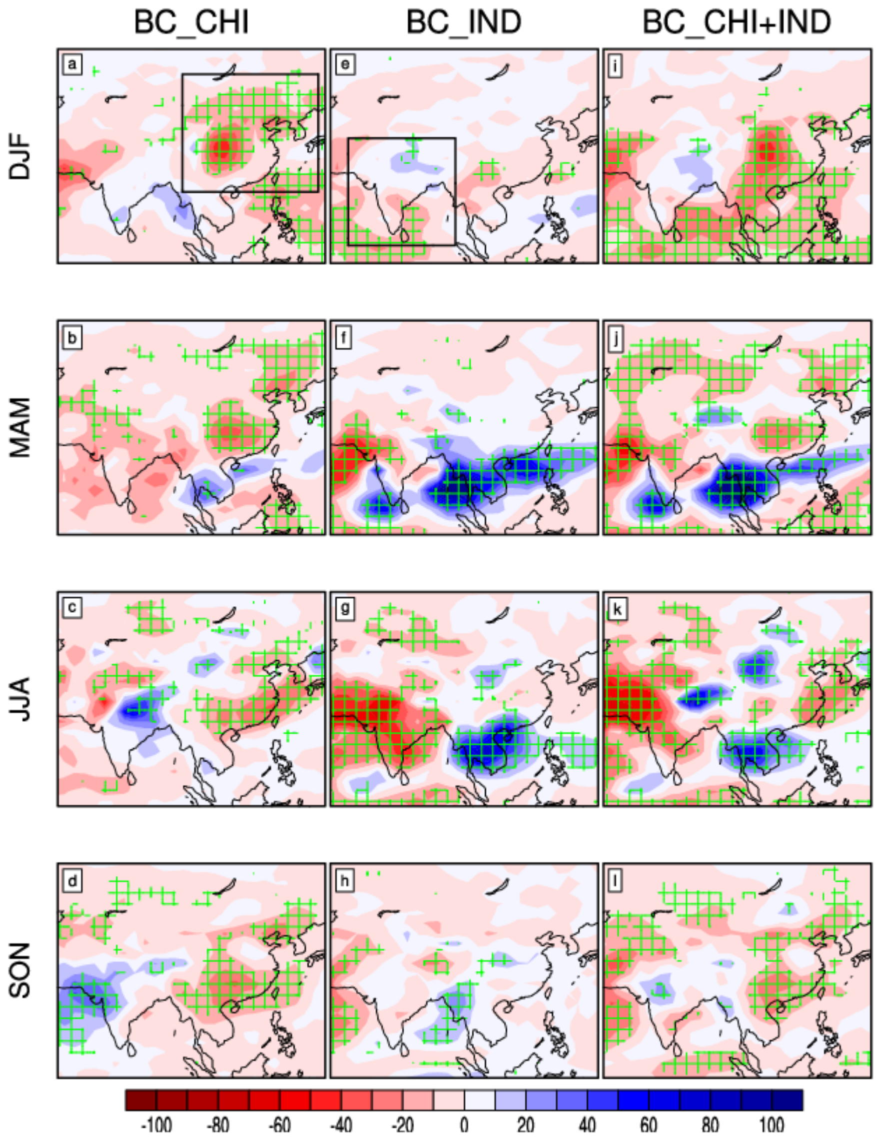

Figure S6. Spatial patterns of precipitation rate responses in (a-d) BC_CHI, (e-h) BC_IND, and (i-l) BC_CHI+IND for four seasons. The green gridlines indicate the regions where the responses are statistically significant above 95% level based on a two-tailed Student's t-test. The black squares highlight the separate region where BC aerosols are perturbed. Unit: %

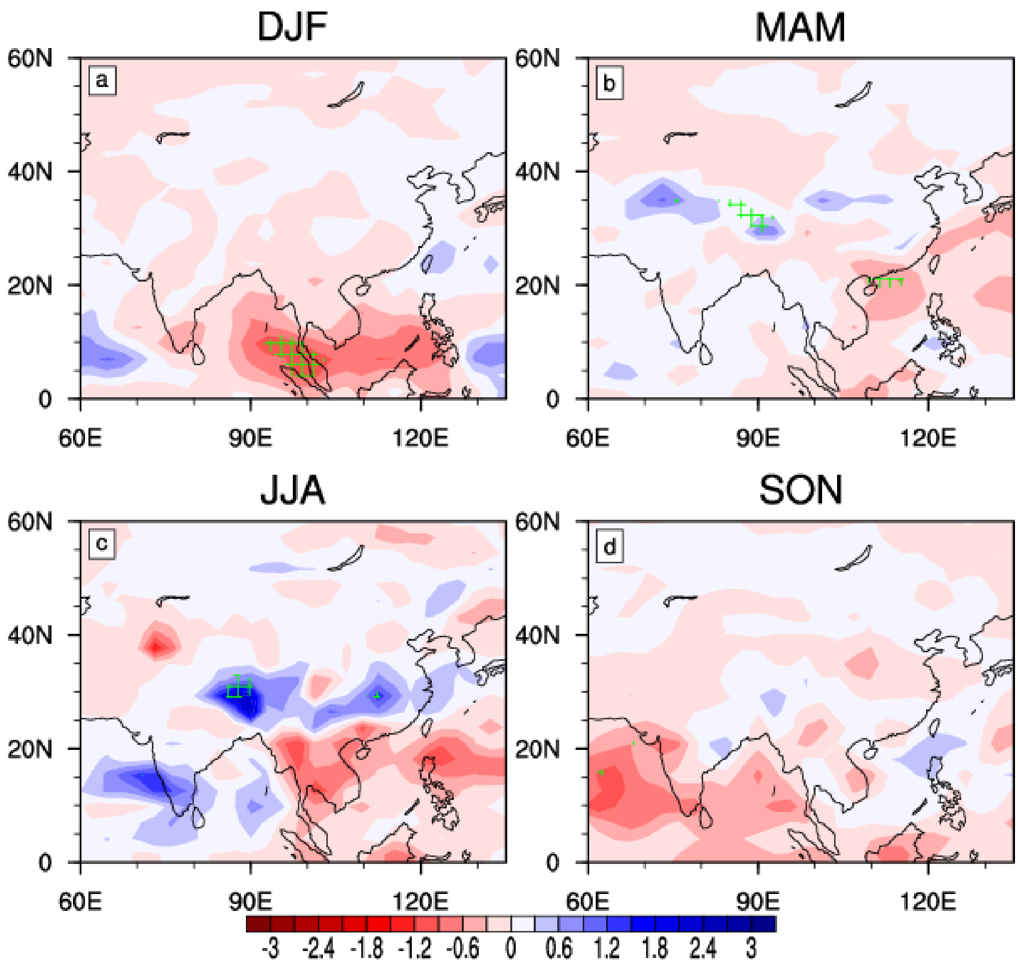

Figure S7. As Figure S5 but for precipitation. Unit: mm/day

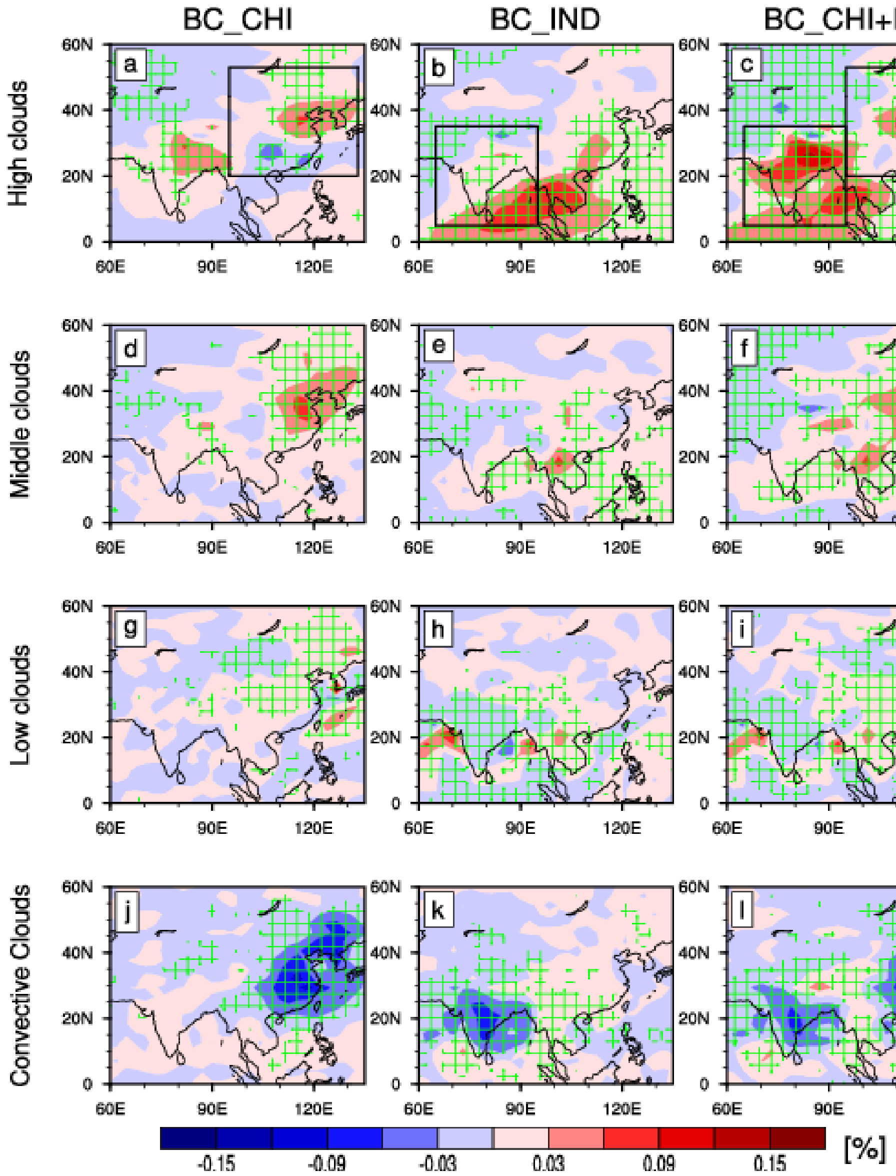

Figure S8. Summer spatial patterns of responses in (a-c) high clouds, (d-f) middle clouds, (g-i) low clouds and (j-l) convective clouds in BC_CHI, BC_IND and BC_CHI+IND. The green gridlines indicate the regions where the responses are statistically significant above 95% level based on a two-tailed Student's t-test. The black squares highlight the regions where BC are perturbed. Unit: %

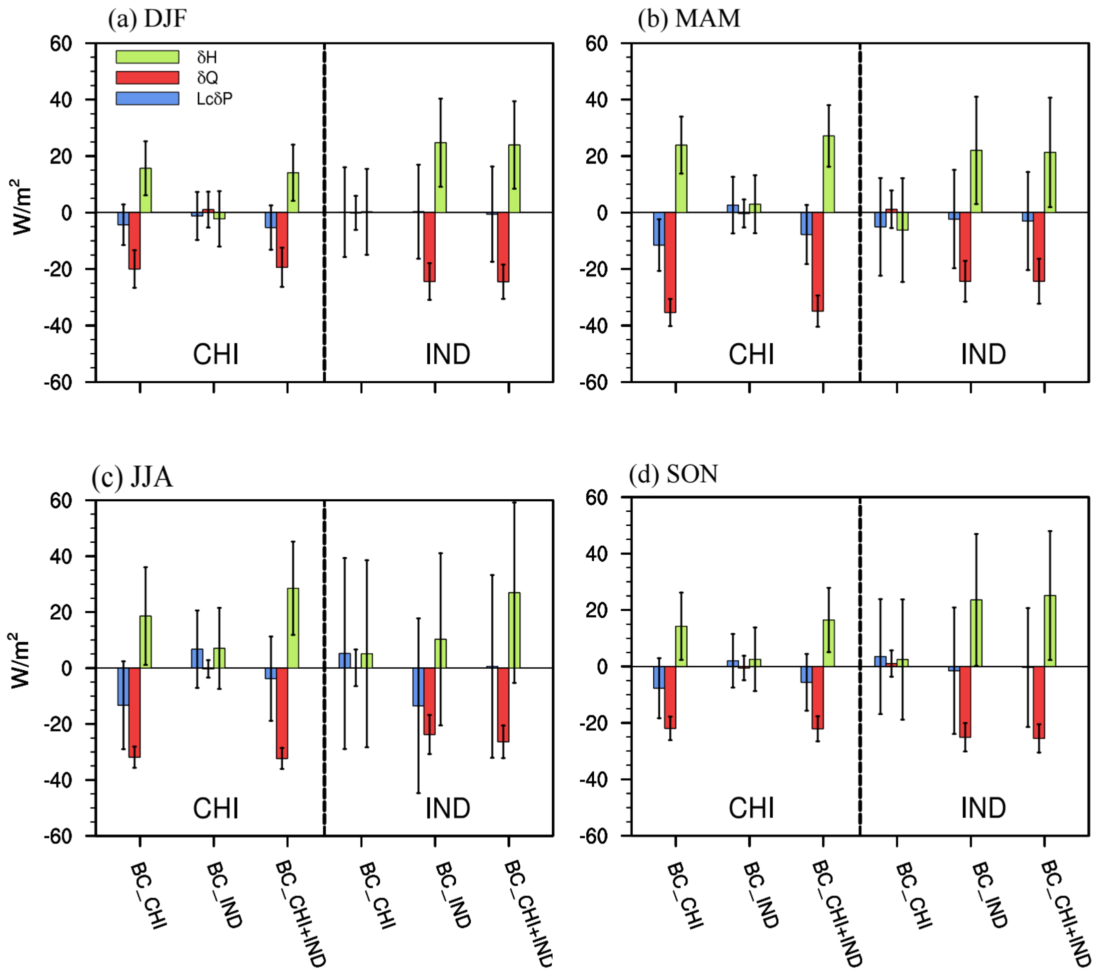

Figure S9. Area-averaged responses of the atmospheric energy budget terms over East China (CHI: 95°E-133°E, 20°N-53°N) and India (IND: 65°E-95°E, 5°N-35°N) in BC_CHI, BC_IND, and BC_CHI+IND. (a) winter, (b) spring, (c) summer and (d) autumn. Error bars represent ±1 standard deviations of the response. Unit: W/m^2

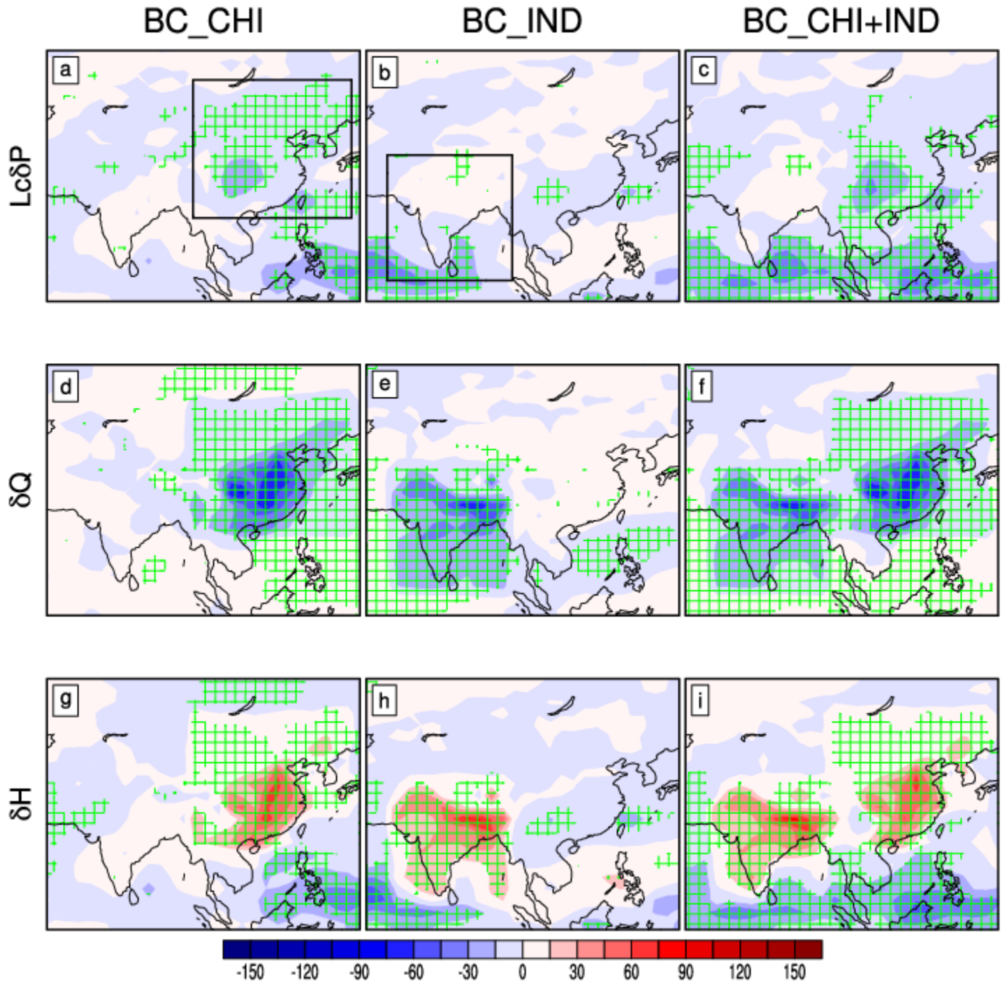

Figure S10. Winter spatial patterns of responses of the atmospheric energy budget terms in BC_CHI, BC_IND, and BC_CHI+IND. (a-c) $L_c\delta P$, (d-f) δQ and (g-i) δH. The green gridlines indicate the regions where the responses are statistically significant above 95% level based on a two-tailed Student's t-test. The black squares highlight the regions where BC are perturbed. Unit: W/m^2

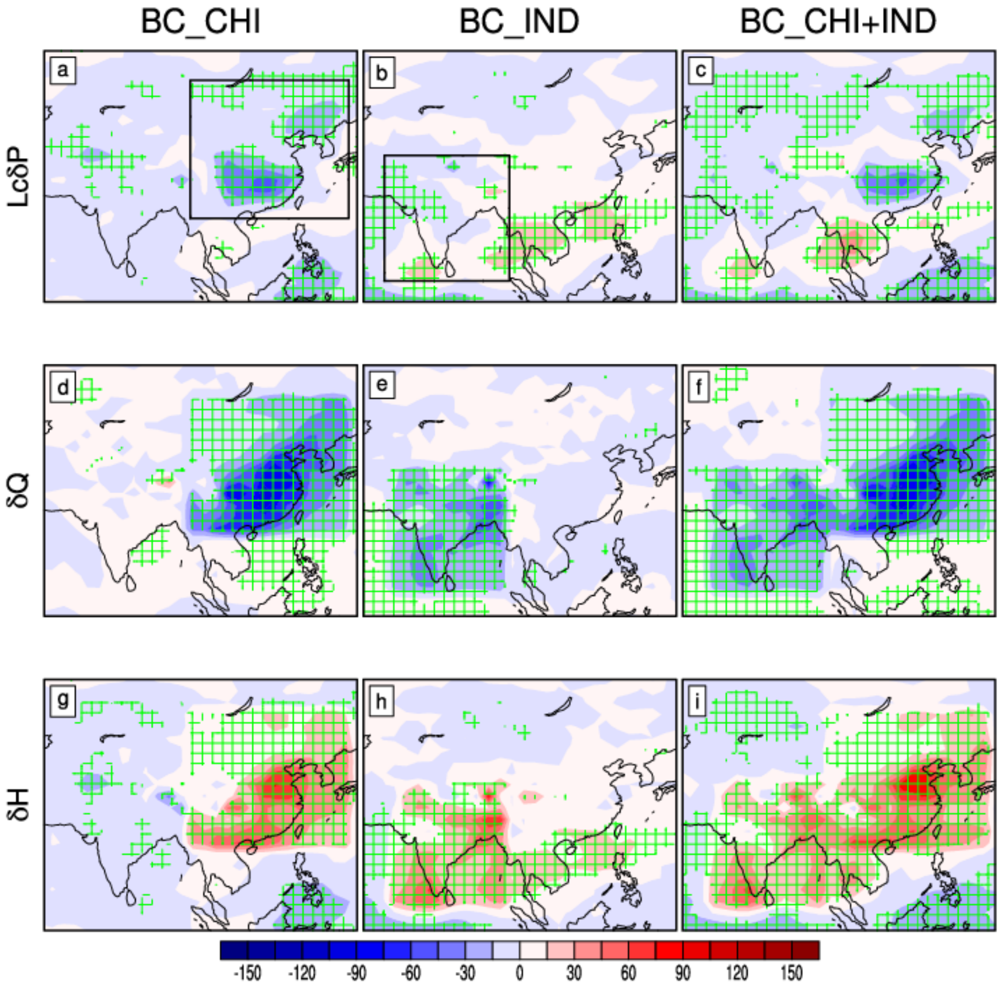

Figure S11. As Figure S10 but for spring.

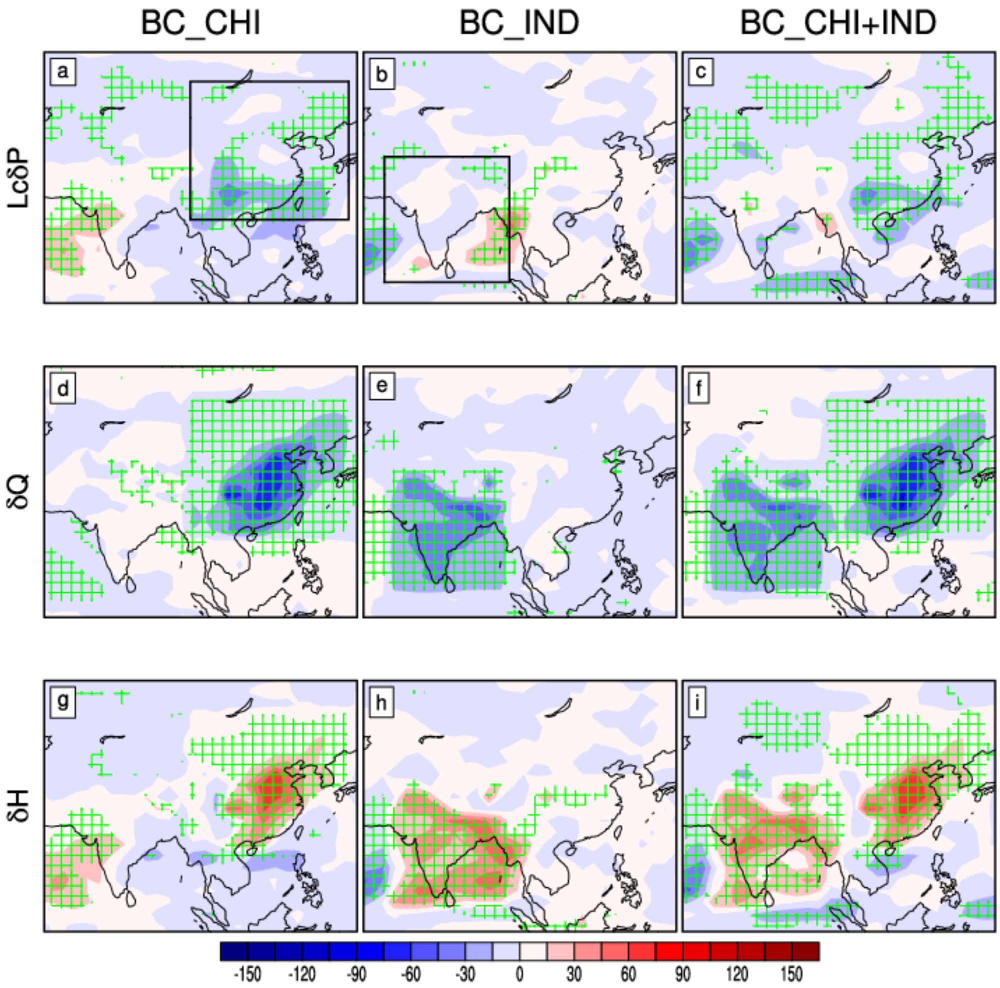

Figure S12. As Figure S10 but for autumn.

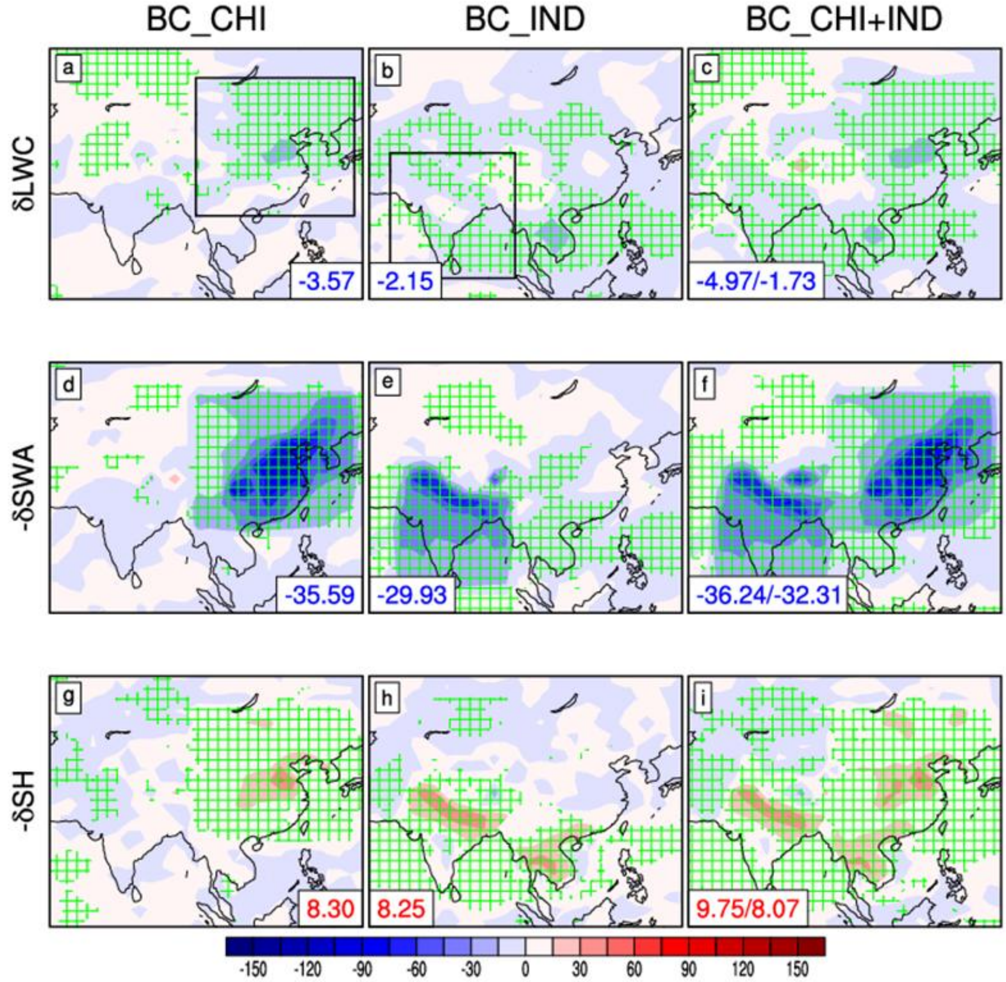

Figure S13. Summer spatial patterns of responses of (a-c) net longwave cooling (LWC), (d-f) net shortwave absorption (SWA), and (g-i) sensible heat flux from the surface (SH) in BC_CHI, BC_IND, and BC_CHI+IND. Area-averaged values over East China and India are given in the lower right corners and lower left corners, respectively. The green gridlines indicate the regions where the responses are statistically significant above 95% level based on a two-tailed Student's t-test. The black squares highlight the regions where BC are perturbed. Unit: W/m^2

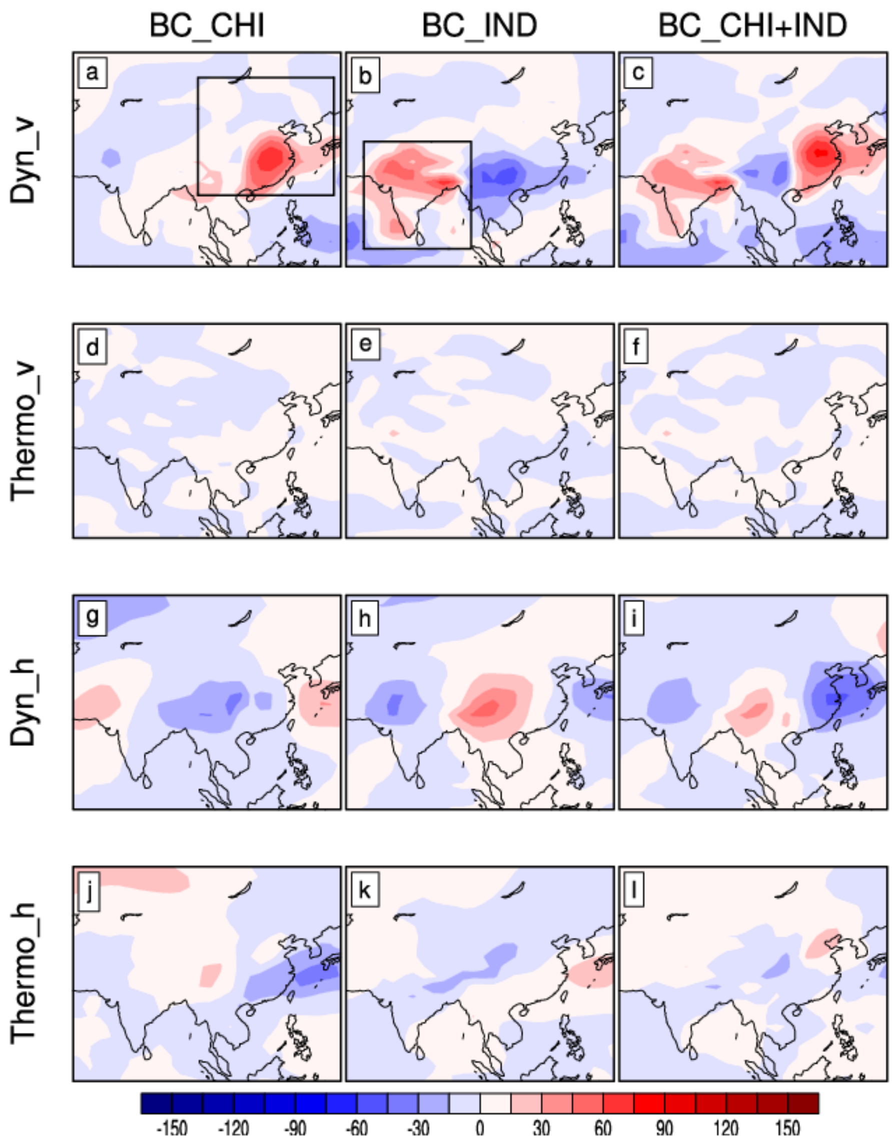

Figure S14. Winter spatial patterns of responses in the four terms decomposed by δH in BC_CHI, BC_IND, and BC_CHI+IND. (a-c) the dynamic components with changes in vertical atmospheric circulations (δH_{Dyn_v}), (d-f) the thermodynamic components with changes in vertical atmospheric circulations (δH_{Thermo_v}), (g-i) dynamic components with changes in horizontal DSE gradients (δH_{Dyn_h}), and (j-l) thermodynamic components with changes in horizontal DSE gradients (δH_{Thermo_h}) The black squares highlight the regions where BC are perturbed. Unit: W/m^2

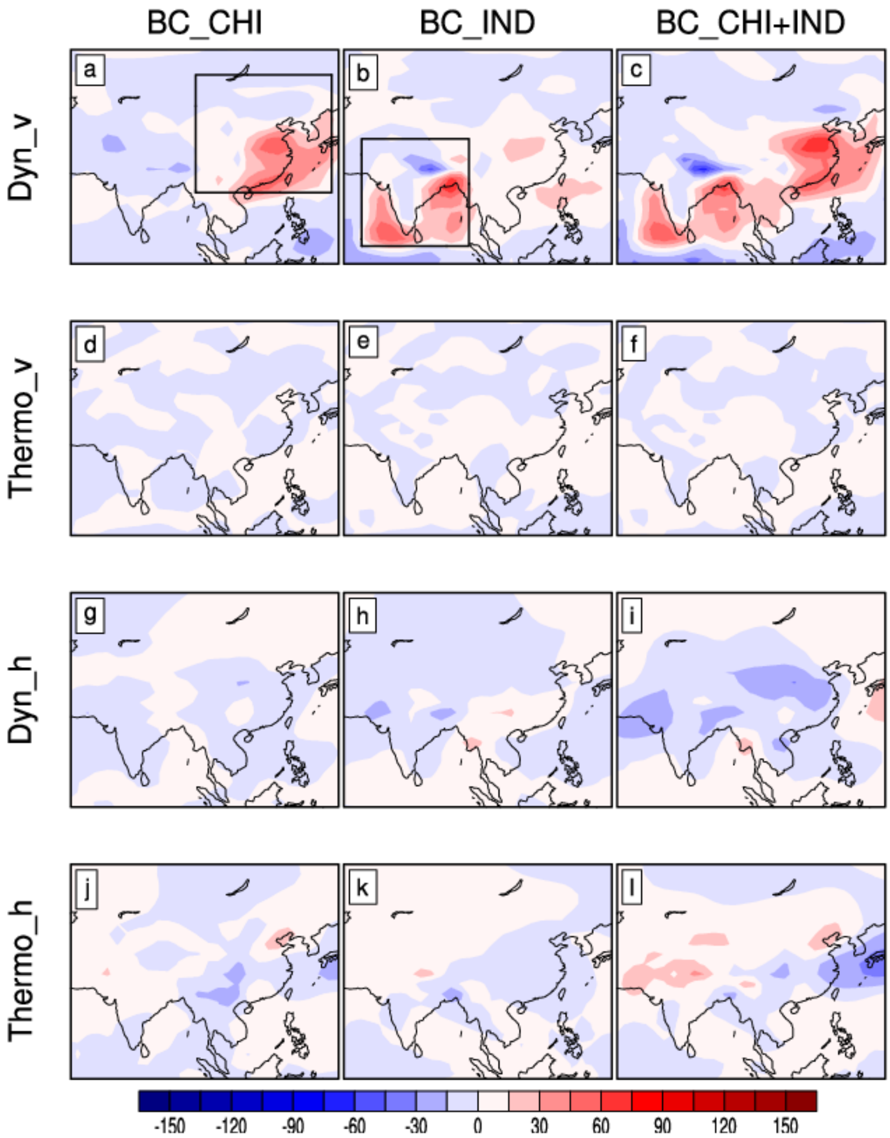

Figure S15. As Figure S14 but for spring.

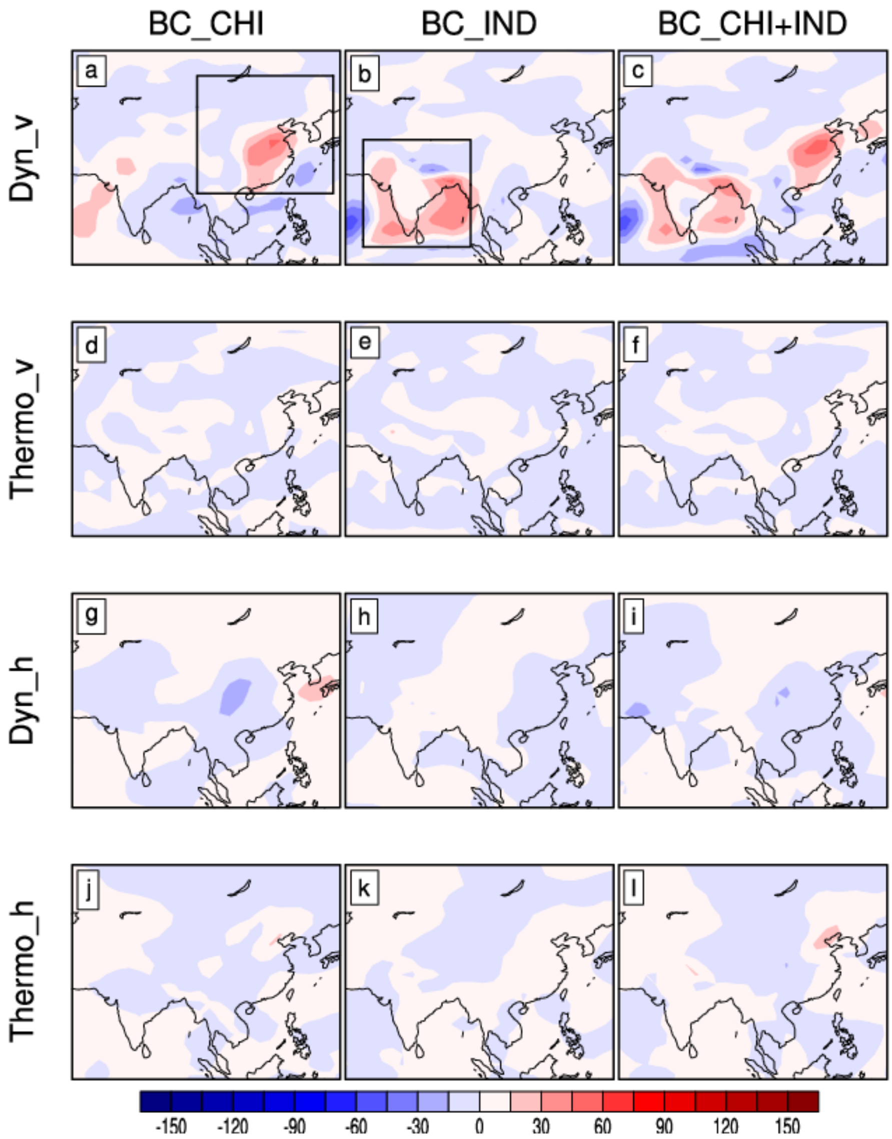

Figure S16. As Figure S14 but for autumn.

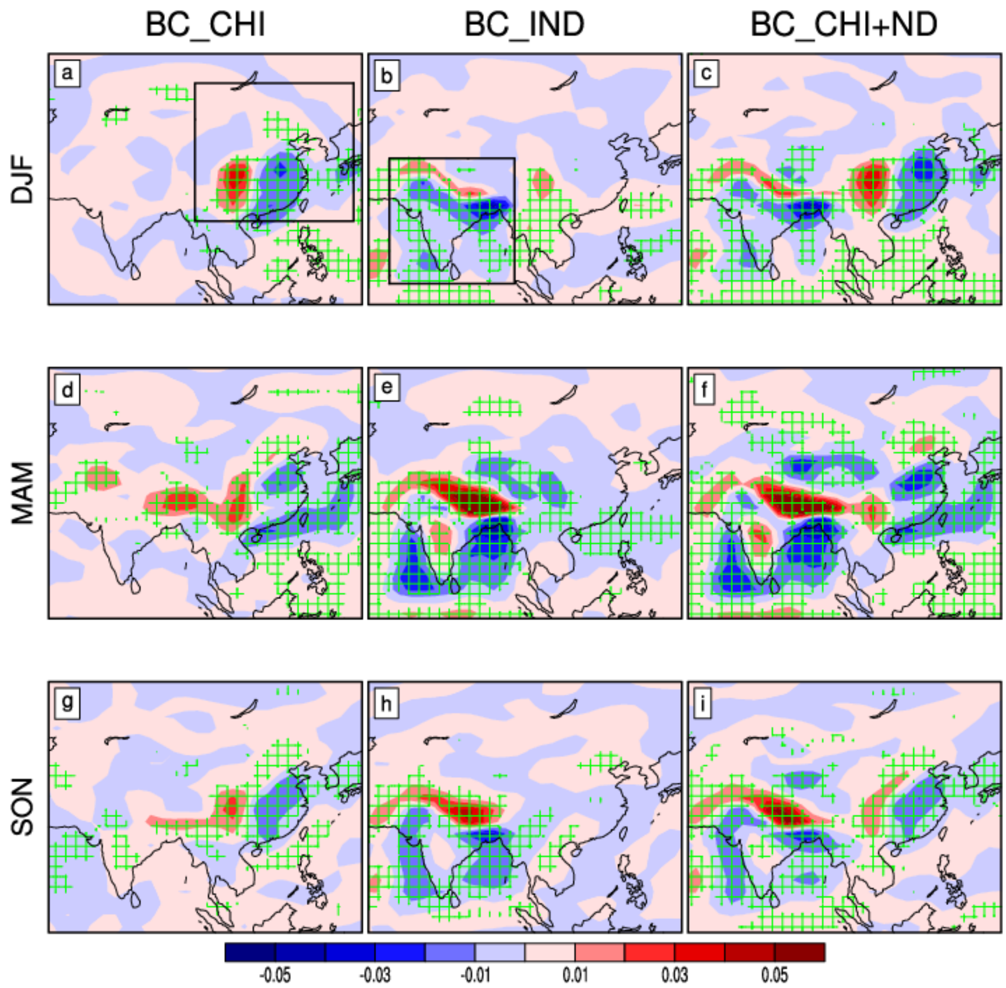

Figure S17. Spatial patterns of responses in Omega at 850 hPa in BC_CHI, BC_IND and BC_CHI+IND. (a-c) DJF, (d-f) MAM, and (g-i) SON. The green gridlines indicate the regions where the responses are statistically significant above 95% level based on a two-tailed Student's t-test. The black squares highlight the regions where BC are perturbed. Unit: Pa/s

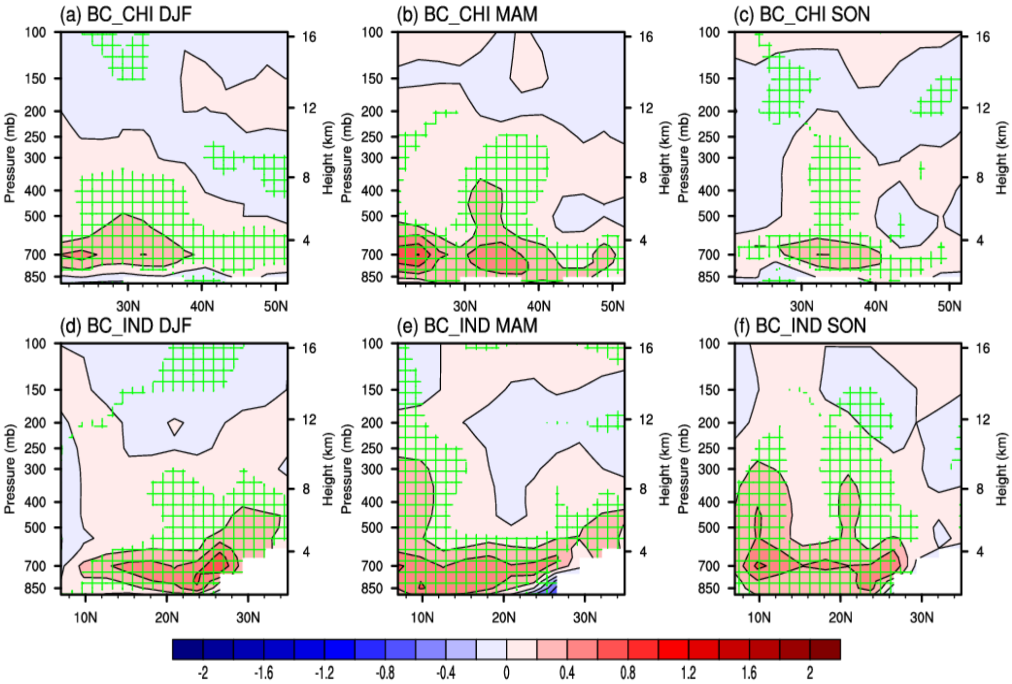

Figure S18. Zonal mean of diabatic heating responses averaged over (a-c) East China (95°E-133°E) for BC_CHI, and over (d-f) India (65°E-95°E) for BC_IND, in DJF, MAM, and SON. The green gridlines indicate the regions where the responses are statistically significant above 95% level based on a two-tailed Student's t-test. Unit: K/day

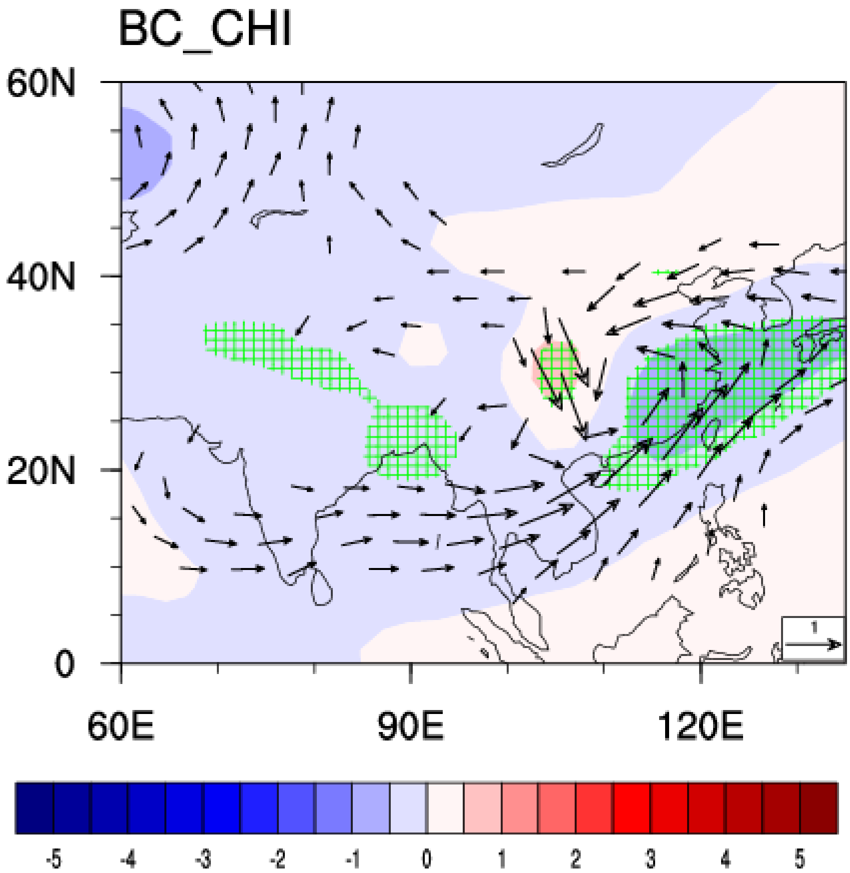

Figure S19. Winter spatial pattern of responses in SLP (Unit: hPa) and horizontal wind at 850 hPa (Unit: m/s) for BC_CHI. The green gridlines indicate the regions where the responses are statistically significant above 95% level based on a two-tailed Student's t-test. Only regions with at least one component of the wind significant above the 95% level are shown.

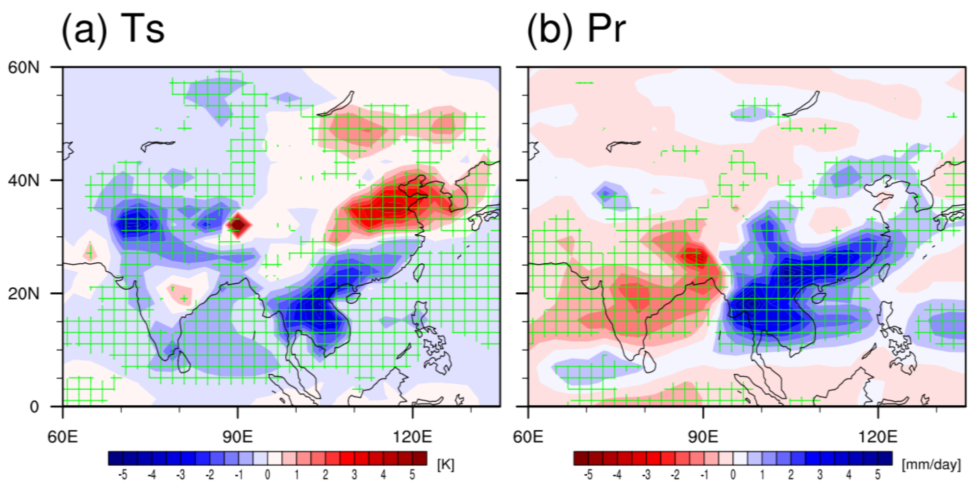

Figure S20. Summer (a) Ts (Unit: K) and (b) precipitation (Unit: mm/day) responses to the dipole pattern measured by a sum of -(BC_CHI-piC) and (BC2-piC). The green gridlines indicate the regions where the responses are statistically significant above 95% level based on a two-tailed Student's t-test.